ESTABLISHING A MULTI-PROXY APPROACH TO ALPINE BLOCKFIELD EVOLUTION IN SOUTH-CENTRAL NORWAY

PHILIPP MARR*, JÖRG LÖFFLER

University of Bonn, Department of Geography, Meckenheimer Allee 166, 53115 Bonn, Gemany
* Corresponding author: marr@uni-bonn.de

ABSTRACT

Blockfields in high latitude mountain areas are a wide spread proxy for glaciation history. Their origin is debated since decades, especially in south-central Norway, where glaciation had a major global climate implication. Some authors explain old blockfield features by protection of cold-based ice, others claim they persisted as nunataks during the LGM (~20 kyr), or were formed throughout the Holocene. In order to clarify the origin of alpine blockfields we established a multi-method approach to combining lichenometry, stratigraphy, granulometry, and geochemistry (XRD, XRF). Our lichenometric dating results in conjunction with our factors indicate landscape stability for at least ~12.5 kyr. Frequent climatic shifts are evident in our profiles by varying color, LOI content and grain sizes. On the basis of geochemical analyses we were able to identify a long-term (chemical) weathering history and in situ blockfield formation. The field evidences and the climatic setting of the study area leave the possibility that our location was not covered by cold-based ice during the Late-Quaternary.

Keywords: glaciation history; Scandinavia; mountains; geochemistry

Received 27 February 2017; Accepted 18 October 2017; Published online 21 November 2017

1. Introduction

For more than 100 years there has been an ongoing debate about the glaciation history of Scandinavia, particularly in south-central Norway (Blytt 1876; Lagerbäck 1988; Mangerud 1991; Nesje et al. 2007). Glaciation history and former ice sheet configurations are important aspects in terms of understanding atmospheric as well as oceanic circulation and temperatures, sea level changes, thermohaline circulation and glacial landform evolution (Winguth et al. 2005; Goehring et al. 2008; Sejrup et al. 2009). The glaciation history with regard to glacial cycles during the Quaternary is fairly known (Mangerud 2004; Linge et al. 2006). However, the knowledge about ice thickness, ice thickness evolution, flow configuration and englacial thermal conditions are very limited (Winguth et al. 2005; Goehring et al. 2008). With the help of relict non-glacial landforms (for discussion see Goodfellow 2007) such as blockfields it is possible to quantify Quaternary glacial erosion, reconstruct landscape development and ice sheet properties (Goodfellow 2007; Ballantyne 2010). Typically, blockfields consist of in situ weathered angular blocks and rocks. The surface rocks frequently cover a soil matrix, mixed with different grain sizes (Rea et al. 1996; Ballantyne 2010). Despite the long debate, the age of blockfields mostly remain ambiguous. Some authors favor the Neogene-origin model (Nesje et al. 1988; Marquette et al. 2004; Fjellanger et al. 2006) where blockfields developed during warmer than present climate. Others claim that blockfields are Quaternary periglacial features (Dredge 1992; Ballantyne 1998; Goodfellow 2012), where blockfields are formed through a combination of physical and chemical weathering, independently from Neogenic influences. The role of blockfields during recent glaciations is dominated by three schools of thought which either claim 1) that blockfields are Holocene features induced by frost shattering or frost sorting (Dahl 1966), 2) blockfield preservation by a cold-based, non-erosive ice sheet (Sugden and Watts 1977; Lagerbäck 1988; Kleman and Borgström 1990; Kleman 1994; Fjellanger et al. 2006) or 3) that blockfields represent ice-free areas (nunataks) within a thin ice sheet configuration with selective glaciations (Nesje et al. 1988, 2007; Nesje and Dahl 1990; Brook et al. 1996; Ballantyne et al. 1997; Landvik et al. 2003).

A mountain over which the above mentioned issues had been discussed is Blåhø (Nesje et al. 1994; Goehring et al. 2008; Strømsøe and Paasche 2011). Previous studies do not include systematical investigations of soil horizons which are an important source of palaeoenvironmatal information. In this study we are combining several methods to provide new information on the glaciation history of Blåhø. Lichenometric dating can be a useful relative dating tool in arctic-alpine environments where organic based dating techniques are not suitable or fail (Trenbirth 2010). Despite of successful application of lichenometric dating (e.g. Matthews 2005), the reliability of the technique is fundamentally questioned (e.g. Jochimsen 1973; Osborn et al. 2015). Certainly, caution has to be paid designing the sampling strategy, and results have to be interpreted carefully. Comprehensive stratigraphic, granulometric and geochemical soil analyses

https://doi.org/10.14712/23361980.2017.18
Marr, P. – Löffler, J. (2017): Establishing a multi-proxy approach to alpine blockfield evolution in south-central Norway
AUC Geographica, 52, No. 2, pp. 219–236
© 2017 The Authors. This is an open-access article distributed under the terms of the Creative Commons Attribution License (http://creativecommons.org/licenses/by/4.0).

help to determine a time integrated weathering history and long-term weathering trends (Strømsøe and Paasche 2011). The role of chemical weathering is believed to be significant since the seminal paper of Rapp (1960). However, only recently the important role of chemical weathering in cold climate conditions is stressed (Hall et al. 2002; Darmody et al. 2005). Moisture availability rather than temperature is the limiting factor of chemical weathering (Hall et al. 2002). The state of chemical weathering gives information about palaeoenvironmental linkages (Nesbitt and Young 1982; Marquette et al. 2004). Chemical weathering is a slow process in cold-dry environments. For soils with advanced chemical alteration a long period of pedogenesis and weathering is indicated (Allen et al. 2001). Chemical processes are important weathering agents, they weather material to fine silt and clay, whereas mechanical weathering mostly produces grain sizes larger than medium silt (Strømsøe and Paasche 2011).

Full scale Fennoscandian ice sheets, covering most of the peninsula were documented within the Quaternary, around 40 glaciation cycles were recorded (Kleman and Stroeven 1997; Kleman et al. 1997). Denton and Hughes (1981) claimed that the ice thickness in Scandinavia reached 2–3 km. However, there are indications that the last major ice sheet was probably thinner than assumed, multi-domed and thinned towards the east (Nesje and Dahl 1990), without reaching all mountain peaks in western Norway (Follestad 2003; Winguth et al. 2005). This is sustained by pre-Quaternary landforms conditioning glacial behavior, where already existing valleys acted as trajectories for new ice flow, leaving high summits untouched (Sugden and Watts 1978). Skåla (1848 m a.s.l.) is thought to have escaped the last glaciation (Brook et al. 1996), Folldalen and mountain plateaus in Dovrefjell are supposed to have been ice free during the Younger Dryas (~12.5 kyr) (Dahl et al. 1997; Mangerud 2004). In concert with this, recent studies show that glaciation histories worldwide differ from previous assumptions, as parts of Greenland and Svalbard were ice-free during extended periods of the Pleistocene and the LGM (Landvik et al. 2003; Schaefer et al. 2016).

The aim of our study was to shed light onto the weathering history of a blockfield at Blåhø by applying a multi-proxy approach, including five different methods. As such, the key contribution of our paper is to correlate blockfield weathering characteristics to glaciation history of south-western Norway.

2. The study area

Blåhø (1618 m a.s.l.) is located in south-central Norway (61°53´51 N, 9°16´58 E) along Gudbrandsdalen between Jotunheimen in the south-east and Rondane in the west (Figure 1). The mountain splits into three lower individual peaks, Rundhø at 1556 m a.s.l., Veslrundhø at 1514 m a.s.l, and Storhøi at 1455 m a.s.l. with gently undulating surfaces (Figure 2). The summit plateau of Blåhø is surrounded by gentle slopes to the north, west and south and a steeper slope towards the east. The summit ridge descends to the east, later splitting towards south-east and north-east. Bedrock outcrops are scarce and frost shattered.

The climatic setting is characterized by relatively strong continentality. With a mean annual air temperature (MAAT) of ~−4 °C (Strømsøe and Paasche 2011) and a mean annual precipitation (MAP) between 300 and 400 mm/yr in the valleys, the area represents one of the driest localities in Norway (Moen 1998). Recent data from permafrost boreholes next to our profiles indicate a mean ground temperature (0.05 m depth) of 0.9 °C and 1.0 °C from 2008 to 2009, respectively 2009 to 2010. The mean ground temperature at 10 m depth was 0.7 °C from September 2008 to August 2010. The snow depth (≥ 5 cm) reached >140–269 days and >140–271 days from 2008 to 2009, respectively 2009 to 2010. In the same time range the active layer thickness reached 7 m to 6 m (Farbrot et al. 2011).

The Precambrian bedrock largely consists of quartz; the summit can be lithologically divided into two parts: meta-conglomerate and meta-sandstone are present at higher, respectively lower slopes (Sigmond et al. 1984; Goehring et al. 2008; Farbrot et al. 2011). The area from the summit to about 1500 m a.s.l. is piled with autochthonous blockfields. The highly weathered and lichen encrusted rock surfaces indicate current surface stability. No signs of glaciofluvial meltwater channels were found. The middle-alpine vegetation on the ridges and peaks is dominated by lichens and graminoids. From 1500 to 1300 m a.s.l. mostly allochthonous blockfields are present (Nesje et al. 1994). On lower slopes exposed bedrock surfaces with clear glacial striations can be found.

In order to test variations of soil horizon and weathering characteristics three pits were manually excavated to log vertical soil profiles (Figure 3). The first (P1) was dug at a side summit of Blåhø (61°54´12 N, 9°16´36 E; 1518 m a.s.l.) with a north north-eastern orientation and an inclination of 4°–6°. This minimizes the likelihood of material removal or addition (Allen et al. 2001). P1 is surrounded by relatively flat topography which is smoothly rising towards the summit in the south and gently sloping towards the other sides. P1 has a depth of 160 cm, eight horizons were labeled from the bottom in ascending order from 0 to 7. On the summit two erratics were identified.

The other two pits (P2a, P2b), 1.5 km west of Blåhø at the south-eastern slope of Rundhø, were labeled to three horizons. The slope is characterized by periglacial patterned ground phenomena (blockstreams) with south-western orientation and 12° inclination (Figure 4). The pit of P2a with a depth of 140 cm is located in the blockstream (61°54´50 N, 9°14´55 E; 1467 m a.s.l.), P2b is 110 cm deep and directly located next to the blockstream

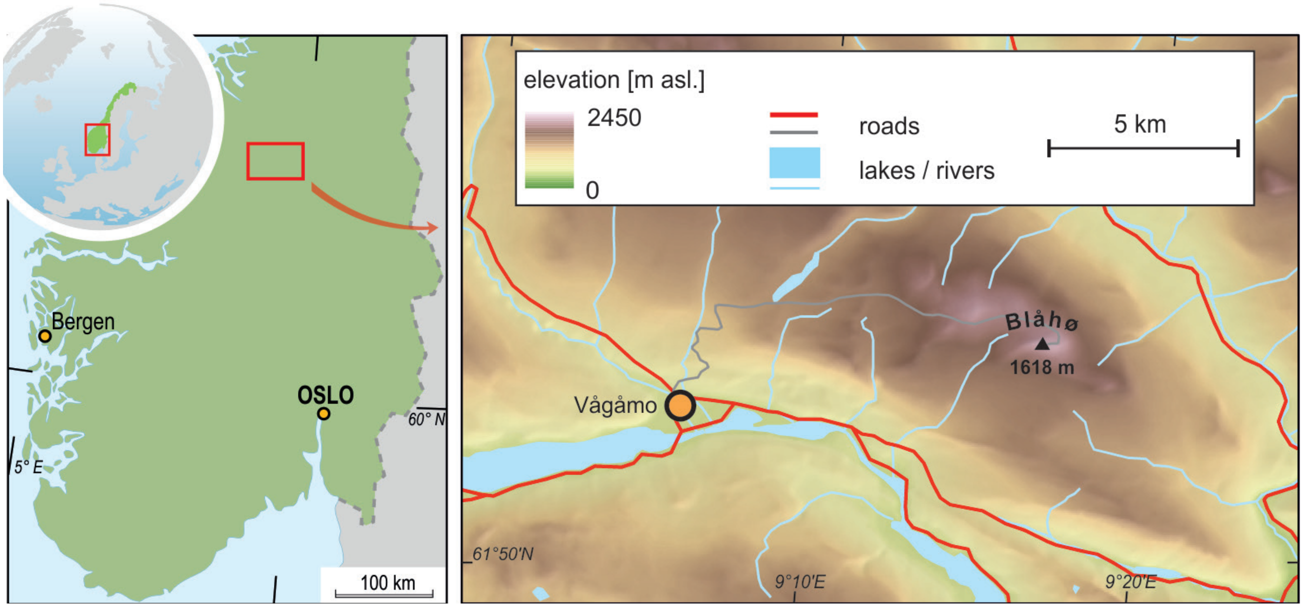

Fig. 1 Map of the study area in south-central Norway; modified after Pape & Löffler (2017).

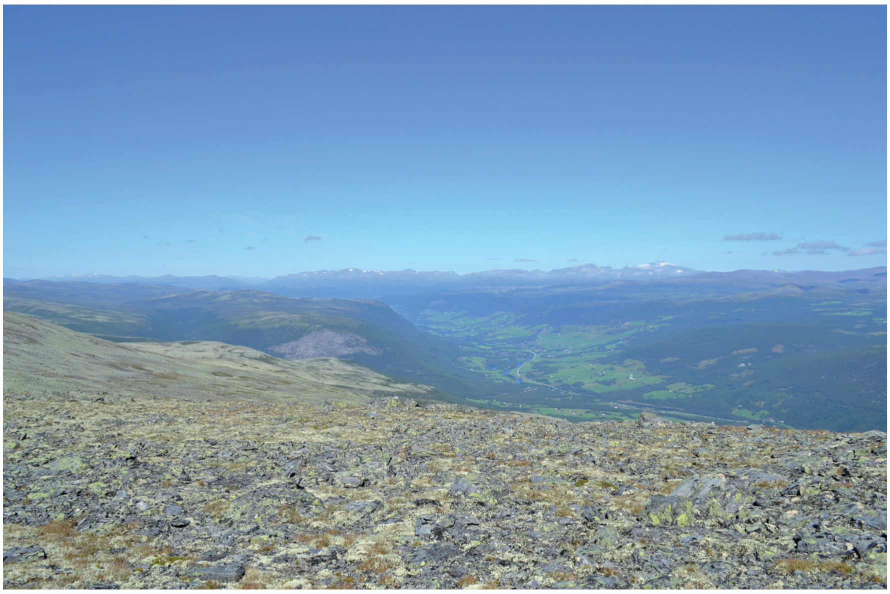

Fig. 2 View from the blockfield towards northwest.

3. Methods

The multi-proxy approach was designed to avoid limitations of single methods and benefit from synergetic effects combining different methods. Estimated surface ages from lichenometric dating can give indications about the surface stability during the late Holocene. Stratigraphical units, in combination with granulometry and organic content; can provide information about climatic circumstances they developed in and past weathering conditions they were exposed to. X-Ray fluorescence (XRF) and X-Ray diffraction (XRD) reveal information about the (chemical) weathering history, weathering indices about on age and provenance of the material.

3.1 Lichenometric dating

In this study the green crutose lichens of *Rhizocarpon subgenus* (often described as *Rhizocarpon geographicum*) are investigated. They are abundant, easily recognizable and have often been used to determine rock surface ages successfully (Trenbirth 2010; Armstrong 2011). Lichens were measured in a sufficient study area of 225 m^2 around the pits (Bradwell 2009). In sum, 72 randomly selected lichens were measured at their longest axis to the nearest millimeter (P1 n = 33, P2 n = 39). The measurements were performed within uniform lithological setting and undertaken by one person within two hours at each site. To ensure measurement consistency, only lichens on near horizontal surfaces on the upper side of stable boulders

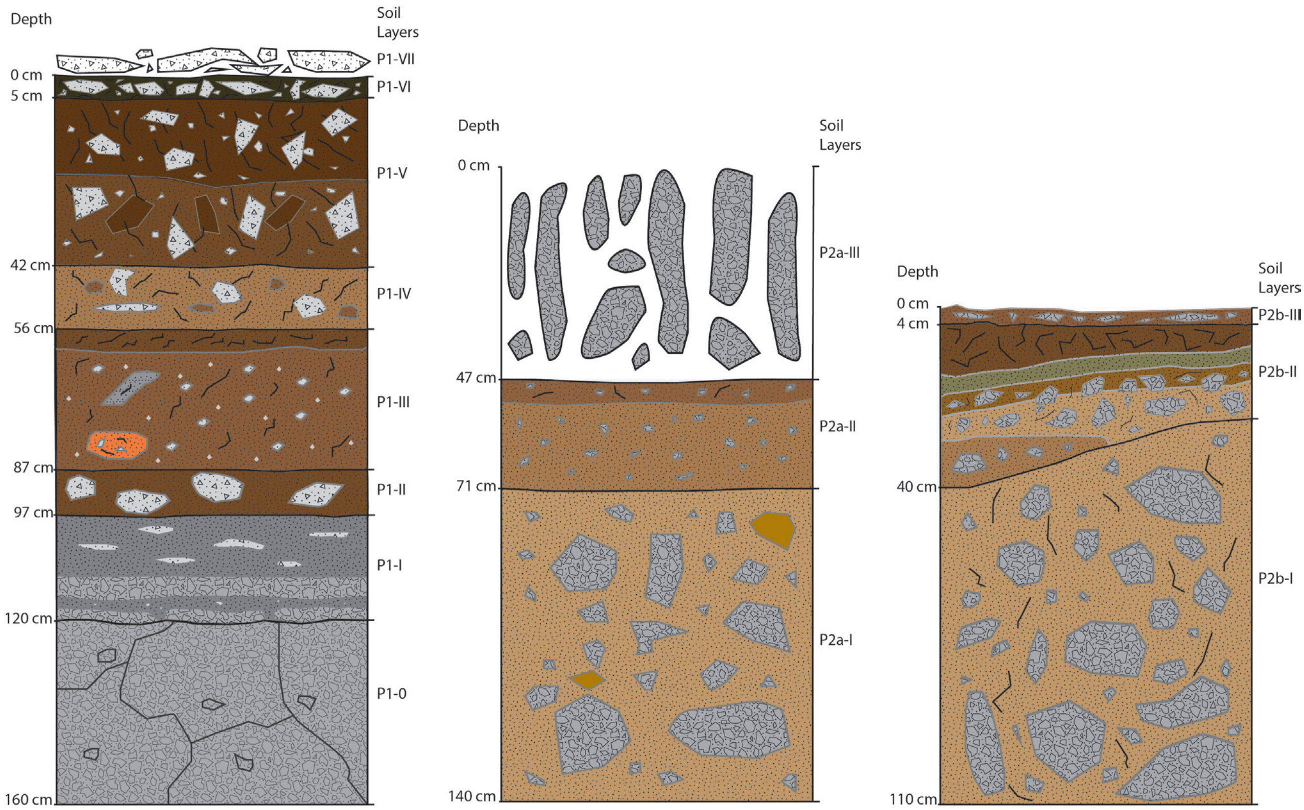

Fig. 3 Schematic stratigraphic profiles of P1 (left), P2a (center), P2b (right).

Fig. 4 View from top of the blockstream towards south.

(> 0.3 m) or on bedrock were measured. It was ensured that all lichens had a mostly uniform inclication towards north (P1) and south (P2). All measured lichens were free of weathering features, (close to) circular and differentiable individuals with no coalesce to other lichens (Figure 5). Standard statistical treatment was carried out (Table 1). The mean of the five largest lichens were used as suggested by many authors (e.g. Shakesby et al. 2004; Matthews 2005). As the rock surface age in this study is of unknown age, the regional lichenometric dating curve from eastern Jotunheimen (Matthews 2005) was used. This has already been applied successfully in south-central Norway (Winkler et al. 2003; Shakesby et al. 2004). No indications for lichen growth variations between regions in southern Norway were found so far (Trenbirth and Matthews 2010). The estimated growth rate for old surfaces in eastern Jotunheimen is 0.45 mm/yr and is applied here due to spatial proximity (Matthews 2005). However, Harris et al. (1987) present growth rates in Jotunheimen of 0.14 mm/yr at 1575 m a.s.l. in Jotunheimen. Growth velocities are negatively affected by cold-dry micro-scale environmental conditions (Beschel 1961; Webber and Andrews

Fig. 5 Lichen measurement (Picture P. Marr).

1973). Hence, the results of this study should be considered as minimal ages (Matthews 1994). Lichens require long colonization time and show nonlinear growth rates (Benedict 1967; Jochimsen 1973). Through prolonged lichen growth it is possible that the present lichens are not original colonizers as mortality rates range between 0.38 and 5.08 % in a 19 year interval (Trenbirth and Matthews 2010; Armstrong 2016). Many climatic and ecological factors influence the behavior of lichen colonization, growth, growth rates and mortality to an uncertain extent.

3.2 Stratigraphy, Granulometry and LOI

Soil horizons were classified at each profile and a mean of 2.8 kilograms of representative bulk samples (including soil and skeleton) were taken from each horizon. All following measurements were carried out with representative samples of each horizon. P1 was divided into eight horizons, P1-VII (surface sample), P1-VI (0–5 cm), P1-V (5–41 cm), P1-IV (42–56 cm), P1-III (56–87 cm), P1-II (87–97 cm), P1-I (97–120 cm), P1-0 (120–160 cm). Each P2a and P2b were labeled with three horizons, P2a-III (0–47 cm), P2a-II (47–71 cm), P2a-I (71–140 cm), P2b-III (0–4 cm), P2b-II (4–40 cm), P2b-I (40–110 cm). The information on color (Munsell 1994), soil matrix, distribution and configuration of rocks were processed into comprehensive illustration (Figure 3). Samples were air dried and the collected soil matrix from each horizon was sieved and divided into fine matrix (< 2 mm) and skeleton fractions (> 2 mm). Organic carbon content was determined by loss on ignition (LOI) at 550 °C as described by Heiri et al. (2001). 5 g of air dried fine matrix was heated to 105 °C for twelve hours and cooled in the desiccator. Subsequently, samples were heated to 500–550 °C in the muffle furnace for ten hours. After cooling in the desiccator, the weight loss was measured and the organic content calculated (in %). Each sample was measured twice. Two microspoons of fine matrix from each horizon were subject to grain size analysis, with a four time repetition measurement each. Samples were prepared according to DIN 18123 and calculated with the Mie-Theory (Markl and Marks 2008). The laser light scattering spectrometer (HORIBA LA-950) was used for granulometric analysis.

3.3 Geochemical analyses

XRF measurements were carried out with the PANalytical Axios FAST spectrometer. Sample preparation followed standard procedures. Fine and skeleton samples from each horizon were analyzed separately. XRD was measured with the Bruker AXS, D8 Advance to identify and quantify primary (quartz, plagioclase, mica, amphibole) and secondary minerals (kaolinite, chlorite and gibbsite) (Marquette et al. 2004; Goodfellow et al. 2009). Results below 10 ppm were excluded from the analysis (Sheldon and Tabor 2009). Diffractograms generated by software applications create semi quantitative data of mineral percentages (Tucker 1996). Illite and muscovite cannot be distinguished in the diffractogram, therefore the superordinate term mica is. The term plagioclase is used to include different feldspar representatives. Site-related geochemical gains and losses in mass transfer can be illustrated by applying the isocon technique. Relating the amount of mobile to immobile elements between bedrock and fine matrix (Grant 2005), based on the assumption that the bedrock is unweathered. Mobile elements in fine matrix such as Sr, K, Mg, Ca and Na are expected to decrease in comparison to the bedrock and drop underneath the immobile element isocon line. Immobile elements as among others Nb, Y, Ti, Th, Si and Al are expected to be similarly modified than the bedrock and located on the line (Grant 2005; Goodfellow et al. 2009).

Weathering indices such as CIA (Nesbitt and Young 1982) and WIP (Parker 1970) were applied to quantify the severity of chemical alteration and/or geochemical differences in soil profiles (Birkeland 1999; Price and Velbel 2003; Darmody et al. 2005). Molecular proportions were used to calculate the indices. The WIP (equation 1) comprises only mobile elements while CIA (equation 2) assumes Al to be immobile. WIP values decrease with increased weathering, CIA behaves vice versa.

$$WIP = \left(100 \times \left[\left(\frac{2Na_2O}{0.35}\right) + \left(\frac{MgO}{0.9}\right) + \left(\frac{2K_2O}{0.25}\right) + \left(\frac{CaO}{0.7}\right)\right]\right) \quad (1)$$

$$CIA = \left(100 \times \left[\left(\frac{Al_2 0_3}{Al_2 0_3 + CaO + Na_2O + K_2O}\right)\right]\right) \quad (2)$$

The Ti/Zr ratio (equation 3) is used to determine the connectivity of the sample to the chemical composition of the parent material (Maynard 1992).

$$\frac{Ti}{Zr} = \frac{\left(\frac{Ti}{Zr_{regolith}} - \frac{Ti}{Zr_{parent}}\right)}{\frac{Ti}{Zr_{parent}}} \quad (3)$$

4. Results

4.1 Lichenometric dating

Histograms for lichen size distribution around P1 and P2 (Figure 6) show bimodal distributions with several peaks, the populations are not normally distributed. The minimum and maximum values and statistical parameters are listed in Table 1. The statistical calculations show comparable mean, median and standard deviation. The values are positively skewed. The majority of lichen diameters vary between 100 and 140 mm. However, six lichens at P1 and seven at P2 have a larger diameter. The mean diameter of all lichens and the five largest lichens are identical at both pits (Table1, Table 5).

Tab. 1 Lichenometric dating statistical results.

	P1	P2
All data		
No. of observations	33	39
Maximum size (mm)	244	235
Minimum size (mm)	47	54
Mean (mm)	118.97	116.31
Median (mm)	110	106
Standard deviation	48.23	45.27
Standard error of the mean	8.4	7.25
Confidence interval of the mean (95%)	17.1	14.68
Skewness	1.19	1.05
Kurtosis	1.1	0.21

4.2 Stratigraphy

The pits show similarities concerning lichen cover, presence of soil horizons, relatively high amount of fine matrix and the absence of till. Key differences are the amount of soil horizons, pits from Rundhø are more disturbed, complicating their interpretation. P1 is characterized by clear soil horizons with distinct color differences and a recurring color pattern from light to dark. The surface horizon P1-VII is represented by mostly angular rocks without structural orientation. Top soil horizon P1-VI has dark brown color (5Y 4/1), the darkest in the profile. P1-V can be subdivided in a dark brown greyish upper part (2.5Y 4/1) and a slightly lighter lower part (2.5Y 5/1). A cryoturbation soil pocket was visible as material from the upper part of the horizon migrated downwards and was deposited in the matrix of the lower lying horizon. Strong root penetration, mixture of big and small, partly angular rocks is apparent. P1-IV has a lighter brown color (5Y 7/3) and high share of skeleton. P1-III has light brown-greyish color (2.5Y 5/3), darkening towards the upper part. It is characterized by small rocks, low amount of roots and the lowest skeleton proportion of the profile (Table 3). P1-II exhibits a brownish color (2.5Y 4/3) with large rocks. A broad color change to grey appears towards P1-I (7.5Y 7/2). The lowest horizon P1-0 is characterized by a light grey color (7.5Y 7/1) and very big, flat rocks dominating the compact matrix with the highest skeleton share. Most likely the bedrock was reached, as it was not possible to dig deeper. Top horizon P2a-III shows big flat rocks, rounded by periglacial processes. P2a-II is characterized by a light brown color (2.5Y 5/4) without big rocks. The upper part has a brown humic layer. P2a-I displays light ochre brown (2.5Y 6/3) with big and small rocks. P2b-III surface horizon has small flat stones within grass patches. The upper part of P2b-II has a humic layer, strong root penetration and mostly light brown color (2.5Y 6/4), darkening towards the lower part of the horizon and gets increasingly heterogeneous. The color of P2b-I changes from a dark brown (2.5Y 4/6) in the upper part to a light brown (2.5Y 5/6) at the bottom, with mostly big rocks.

4.3 Granulometry and LOI

A repetitive trend is observable in the profile as the declining amount of silt from P1-I to P1-II and P1-IV to P1-V are comparable (Table 2). From P1-I there is an increase of the sand fraction, peaking at P1-II, subsequently declining until P1-IV where values are comparable to P1-I. From P1-IV to P1-VI silt values again decrease whereas sand is increasingly dominating. The grain size distribution of P2a is characterized by an increasing sand share with depth, in contrast to all other profiles, the relatively high amount of clay which increases with depth. The grain size distribution of P2b shows

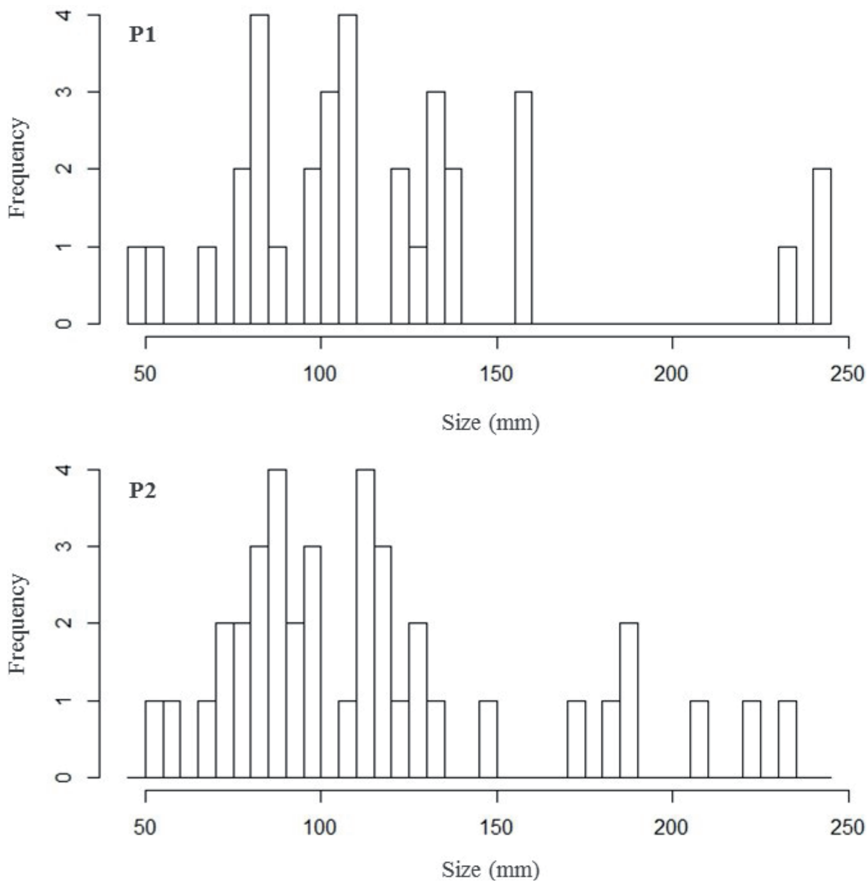

Fig. 6 Histograms plotted with a class size of 5 mm with data from P1 (top) and P2 (bottom).

Tab. 2 Grain size distribution of fine matrix from Blåhø and Rundhø.

	Grain size (%)*							
Sample	**clay (<2 µm)**	**f silt (2–6.3 µm)**	**m silt (6.3–20 µm)**	**c silt (20–63 µm)**	**f sand (63–200 µm)**	**m sand (200–630 µm)**	**c sand (630–2000 µm)**	**clay/silt ratio**
P1-VI	0.64	5.83	20.50	33.82	15.16	13.47	10.59	0.011
P1-V	0.36	5.26	23.49	44.25	20.35	5.02	1.29	0.005
P1-IV	0.32	6.08	30.10	44.86	16.43	2.20	0	0.004
P1-III	0.34	5.06	23.17	43.03	18.93	6.19	3.27	0.005
P1-II	0.45	3.99	17.28	43.68	21.90	8.39	4.32	0.007
P1-I	0.43	6.48	28.77	42.98	15.26	3.56	2.52	0.006
P1-0	0.73	7.61	27.71	39.13	15.16	6.86	2.81	0.010
P2a-II	0.88	5.60	15.56	38.12	31.41	6.95	1.48	0.015
P2a-I	1.81	3.55	6.27	27.77	36.65	21.36	2.59	0.048
P2b-II	1.30	5.10	11.39	32.48	29.04	13.57	7.12	0.027
P2b-I	1.14	3.59	8.04	33.94	33.22	14.69	5.37	0.025

* Grain size fractions: f, fine; m, medium; c, coarse

no distinct pattern. The clay/silt ratios from all samples are low (≤ 0.14).

The LOI fine matrix analyses of P1, P2a and P2b show generally low values (Table 3). The LOI values of all profiles increase towards the surface. P1 shows a deviation from this trend as it peaks first at P1-III, subsequently values decrease and consecutively rise to the peak at P1-VI.

4.4 Geochemical analyses

The results of the major element analysis from fine matrix and skeleton samples show strong similarities, skeleton samples, however, show higher variability (Table 3). It is difficult to identify trends for P2a and P2b as their horizontal zonation is limited and horizons incorporate more heterogeneous material. The comparison of

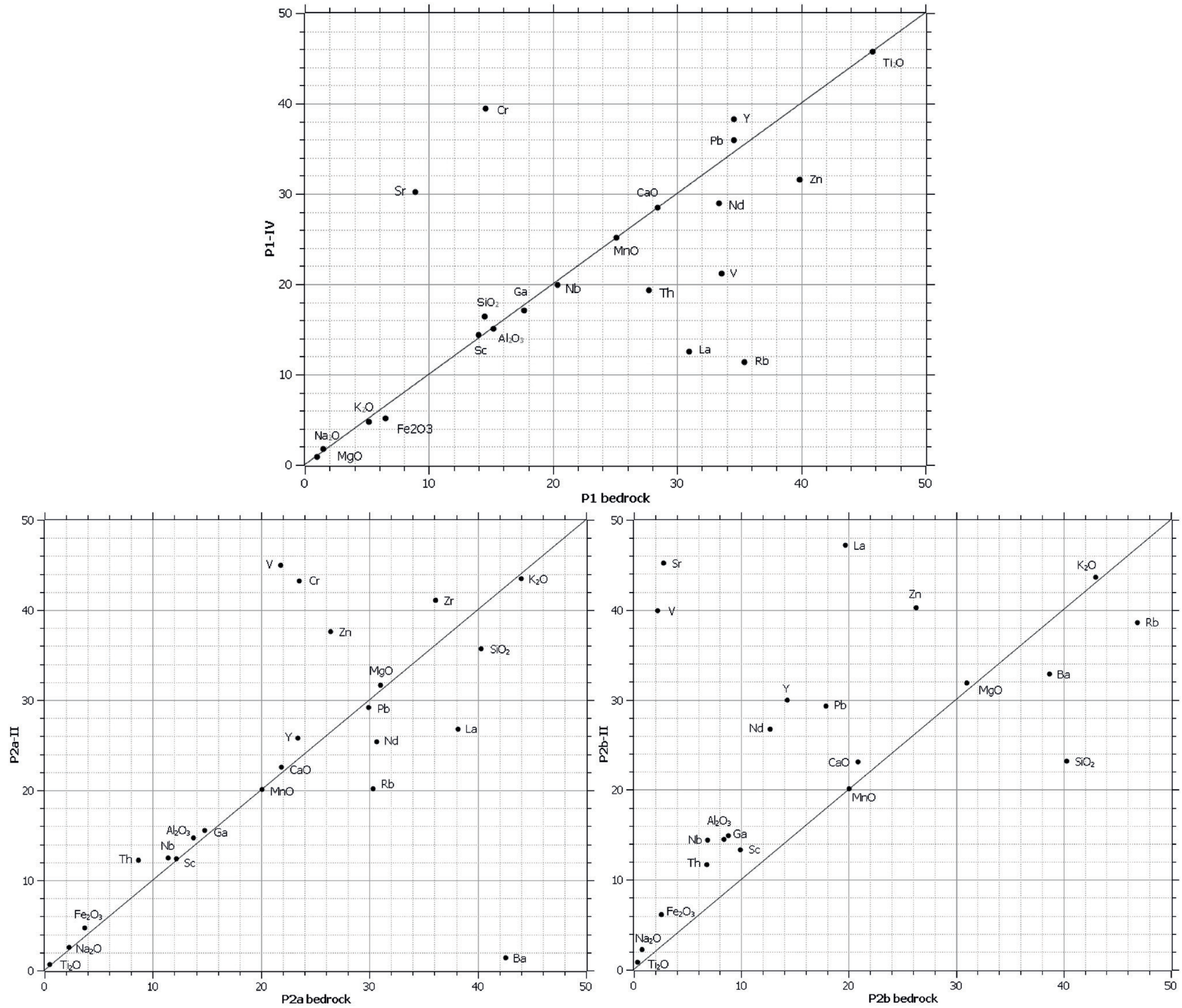

Fig. 7 Isocon plots of element and mineral alteration between fine matrix and bedrock (P1-0, P2a-I, P2a-I) of Blåhø and Rundhø. The diagonal represents the immobile element isocon line. Elements above the line show a concentration increase, elements below were depleted. Element concentrations were scaled to fit in the plots.

geochemical gains and losses between fine matrix with skeleton samples with the isocon technique is illustrated in Figure 7. The displayed trends are comparable to other fine matrix and rock samples within the sites. The values of Ti, Na, Mn, Mg and K from all profiles are similarly altered and located on the isocon line. Rb was depleted in all profiles, whereas P2a/P2b samples show more similarities in enrichment and depletion of elements in comparison to P1.

In Figure 8, the values of weathering indices are plotted with soil horizons. There is little variability in the CIA results of fine matrix and skeleton samples of P1, except for P1-II and P1-IV where the fine matrix shows higher values than skeleton. The WIP values are in the range between 55.1 (P1-V skeleton) and 74.9 (P1-VII skeleton). The calculated Ti/Zr results are −0.2 (P1), 0.5 (P2a) and 0.1 (P2b).

Most trace elements show similar trends at P1. P1-IV is a point where trace elements in fine matrix show changing behavior (Table 3). Subsequently, a phase of stability of the fine matrix samples occurs after depletion from the surface. Many skeleton values show changes from P1-IV to P1-V, with an enrichment of most trace elements. The values generally show little variability, except surface and bottom horizons often show exceptional values. The fine matrix samples of P2a and P2b show limited variation. The skeleton values of P2a mostly increase from P2a-III to P2a-II and subsequently decline downwards. Generally skeleton values of P2b show more variability than fine matrix.

XRD data illustrate primary minerals in all samples. Clay minerals (Table 4) were found in fine matrix samples of P2a and P2b. Quartz is the dominant mineral in most horizons, followed by mica and plagioclase. The skeleton samples show more complex mineral distribution with more variations than fine matrix samples. At P2a and P2b more quartz is present in the fine matrix samples.

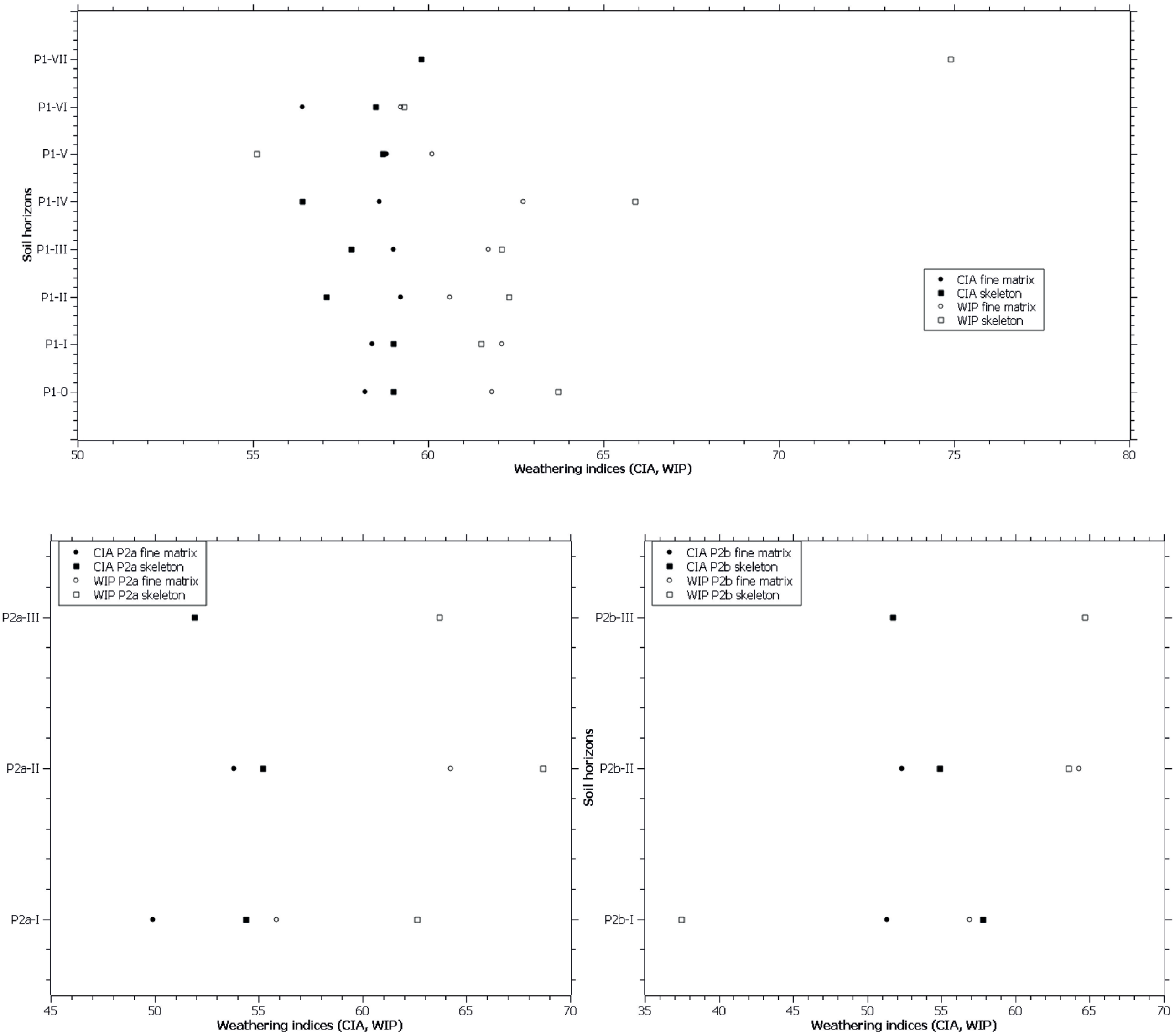

Fig. 8 Weathering indices (WIP and CIA) of all profiles (P1, P2a, P2b) with depth. The indices were calculated for fine matrix (< 2mm) and skeleton fractions (> 2mm).

5. Discussion and conclusion

5.1 Weathering characteristics, geochemical distribution and profile properties

The information on palaeoenvironments conveyed from soils varies in accuracy due to the nature of horizons and the periods surveyed. Therefore, the results must be interpreted carefully. Our XRD and XRF analyses, granulometric results, and weathering indices indicate that chemical weathering has strongly modified the investigated soils. The suggested indicators for chemical weathering by Gouveia et al. (1993) and Goodfellow et al. (2009) are element mobility and low plagioclase values which are present in our profile. Element mobility is reflected in the relationship between silica and iron is an indicator for chemical weathering (e.g. Birkeland 1999). All samples show a fairly strong non-linear relationship (Figure 9; $R^2 = 0.63$; $\alpha < 0.01$), indicating gradual leaching of more mobile elements as silica in comparison to the more stable iron element (Birkeland 1999; Strømsøe and Paasche 2011). With progressed weathering high iron concentrations will be opposed by low silica values. The immobility of many mobile elements is likely connected to the longevity of weathering processes which reach quasi-equilibrium where the rate of chemical weathering is constant but low at present (Strømsøe and Paasche 2011).

Accumulated quartz in the fine matrix in comparison to skeleton samples can be explained by long-term in situ physical weathering. Our Ti/Zr results display negligible divergence between bedrock and soil matrix and support in situ formation (Strømsøe and Paasche 2011). In contrast to Ballantyne's (2010) assumption that soil horizons are usually absent in blockfields, they are well developed in our profiles. This also points to long-term and intense chemical weathering. WIP ratios of P1-V and P2b-I are

Tab. 3 Concentration of major elements (%), trace elements (ppm) and material size (%) from fine matrix and skeleton samples.

		Size (%)		Major Elements (%)										
Sample	**Type**	**<2mm**	**>2mm**	*SiO_2*	*Al_2O_3*	*Fe_2O_3*	*MnO*	*MgO*	*CaO*	*Na_2O*	*K_2O*	*TiO_2*	*LOI*	Total
P1-VI	Sediment	26	74	68.07	13.21	5.31	0.09	0.72	1.44	1.65	4.51	0.69	3.78	95.69
P1-V	Sediment	45	55	67.24	14.55	4.95	0.10	0.82	1.34	1.77	4.49	0.67	2.86	96.46
P1-IV	Sediment	28	72	66.38	15.05	5.18	0.10	0.89	1.43	1.75	4.76	0.69	2.37	96.75
P1-III	Sediment	57	43	66.81	15.04	5.27	0.12	0.89	1.38	1.76	4.65	0.68	2.80	97.11
P1-II	Sediment	35	65	68.00	14.81	5.13	0.10	0.87	1.30	1.77	4.54	0.65	2.66	97.62
P1-I	Sediment	32	68	66.89	14.93	5.38	0.10	0.86	1.47	1.74	4.70	0.69	2.15	97.33
P1-0	Sediment	17	83	67.17	14.81	5.23	0.10	0.85	1.48	1.78	4.63	0.68	2.07	97.18
P1-VII	Skeleton			65.12	16.68	5.08	0.09	1.07	0.75	1.97	6.11	0.67	2.04	97.54
P1-VI	Skeleton			68.02	14.46	4.91	0.12	0.87	1.56	1.45	4.66	0.72	2.05	97.17
P1-V	Skeleton			67.23	13.62	6.80	0.12	0.76	1.51	1.18	4.51	0.84	1.96	97.09
P1-IV	Skeleton			67.15	14.95	5.28	0.09	0.75	1.41	2.76	4.10	0.70	1.76	97.65
P1-III	Skeleton			68.38	14.70	4.31	0.11	0.79	1.43	2.00	4.46	0.63	1.92	97.25
P1-II	Skeleton			68.96	14.57	5.83	0.12	0.77	1.60	1.87	4.57	0.73	1.83	99.69
P1-I	Skeleton			68.16	14.38	4.59	0.08	0.85	1.05	1.88	4.61	0.64	1.97	96.70
P1-0	Skeleton			64.50	15.21	6.54	0.11	1.01	1.40	1.48	5.15	0.77	2.14	96.61
P2a-II	Sediment	43	57	65.67	14.67	4.71	0.09	1.67	2.54	2.56	3.48	0.64	2.91	96.49
P2a-I	Sediment	64	36	71.01	12.57	4.77	0.09	1.63	3.30	2.45	2.40	0.76	1.57	99.56
P2a-III	Skeleton			70.63	13.51	3.94	0.08	1.03	2.25	2.93	3.31	0.44	1.55	98.40
P2a-II	Skeleton			65.23	15.24	4.49	0.10	1.45	2.03	2.27	4.54	0.64	2.13	96.37
P2a-I	Skeleton			70.30	13.73	3.70	0.07	1.05	1.87	2.24	4.04	0.47	1.72	97.80
P2b-II	Sediment	43	57	63.18	14.50	6.13	0.11	1.88	3.10	2.20	3.64	0.79	3.69	95.53
P2b-I	Sediment	36	64	67.98	12.90	4.63	0.08	1.56	2.94	2.43	2.67	0.70	2.14	96.42
P2b-III	Skeleton			66.90	13.92	5.59	0.09	1.36	2.93	1.79	4.35	0.70	1.81	97.63
P2b-II	Skeleton			68.23	14.33	4.54	0.08	1.17	2.08	2.09	4.21	0.64	1.95	97.84
P2b-I	Skeleton			80.26	8.36	2.59	0.04	1.00	0.88	0.76	3.00	0.35	1.32	97.49

	Trace Elements (ppm)																
Sample	Sc	V	Cr	La	Nb	Pb	Zn	Ga	Th	Y	Nd	Mn	Ba	Ce	Zr	Rb	Sr
P1-VI	11	47	15	44	18	39	44	13	12	32	29	569.9	621.3	79.1	335	132	144.8
P1-V	13	57	17	51	19	35	58	17	19	37	30	687.8	842.5	113.2	475.4	170	165.6
P1-IV	14	61	49	53	20	36	62	17	19	38	29	717.3	894.7	130.8	455.8	181.4	170.2
P1-III	15	59	17	61	20	36	60	17	20	38	41	698.1	869.1	121	458.2	176.4	168.1
P1-II	12	59	17	55	18	36	57	16	15	34	32	675.4	858.5	100.5	422.1	172	163.9
P1-I	13	60	15	54	20	36	63	17	18	39	34	732.2	866.7	127.4	508.1	176.4	173.8
P1-0	14	59	20	45	20	37	61	17	20	39	38	741	858.5	163.1	430.8	176.7	173
P1-VII	14	39	32	23	17	24	53	16	21	30	16	514.3	798.7	57.7	218.9	186.4	53.3
P1-VI	14	59	28	36	21	41	60	17	17	36	18	720.5	869.3	78.9	387.5	177.8	197.4
P1-V	15	69	52	55	22	43	62	16	23	35	20	838.4	834.6	150.3	481.6	175.5	185.5
P1-IV	10	54	24	48	20	37	53	17	24	31	19	631.7	730.5	105.2	363	156.4	171.5
P1-III	12	49	20	48	19	38	53	16	19	37	25	643.1	818.7	91.7	366.1	167	184.7
P1-II	15	58	25	46	24	32	58	17	16	42	22	680.8	817.5	65.5	309.2	173.1	144.9
P1-I	13	58	19	49	22	30	59	16	18	48	32	592.6	829.2	163.7	381.7	175.5	117.2
P1-0	14	74	25	71	20	35	70	18	28	35	33	804.6	936	135.5	310.4	205.4	148.9
P2a-II	12	65	53	37	13	29	58	16	12	26	25	617.8	761.4	66.9	251.1	120.2	250.6
P2a-I	15	74	66	45	15	28	46	13	9.4	34	30	598.2	599	66.6	466.2	74.4	317.2
P2a-III	11	48	32	42	10	37	54	15	8.1	22	25	559.3	686	56.5	164.4	111.1	252
P2a-II	15	58	34	42	14	28	63	17	11	25	20	536.9	929.6	54.2	248.8	151.5	196.6
P2a-I	12	42	34	48	11	30	46	15	8.7	23	31	482.7	802.6	57.9	246.1	130.3	199.7
P2b-II	13	70	60	47	14	29	50	15	12	30	27	598.8	642.9	80	367.8	88.6	277.4
P2b-I	13	68	59	40	15	28	50	14	10	33	32	609.6	636	75.4	413.1	86.5	287.6
P2b-III	12	50	30	48	15	33	50	14	12	29	30	543.9	752.3	67.7	236	109.8	275.2
P2b-II	13	60	37	45	14	31	53	16	15	25	27	588.1	888.1	66.9	316.6	131.8	243.9
P2b-I	9.9	32	18	20	6.9	18	36	8.8	6.8	14	13	305.5	648.7	29.7	122.5	96.9	69.5

Tab. 4 Composition of minerals (%) from fine matrix and skeleton samples.

Mineral Composition (%)						
Sample	*Type*	*Quartz*	*Mica*	*Plagioclase*	*Amphibole*	*Kaolinite/Chlorite*
P1-VI	Sediment	67	21	12		
P1-V	Sediment	48	34	17		
P1-IV	Sediment	41	46	13		
P1-III	Sediment	53	37	9		
P1-II	Sediment	47	36	17		
P1-I	Sediment	49	34	17		
P1-0	Sediment	51	34	15		
P1-VII	Skeleton	48	29	23		
P1-VI	Skeleton	49	37	14		
P1-V	Skeleton	53	37	10		
P1-IV	Skeleton	47	22	30		
P1-III	Skeleton	42	38	20		
P1-II	Skeleton	39	38	23		
P1-I	Skeleton	56	27	17		
P1-0	Skeleton	34	46	20		
P2a-II	Sediment	51	23	25	1	1
P2a-I	Sediment	66	9	22	2	1
P2a-III	Skeleton	58	13	28		
P2a-II	Skeleton	43	30	27		
P2a-I	Skeleton	54	23	23		
P2b-II	Sediment	57	13	27	1	1
P2b-I	Sediment	65	14	19	1	1
P2b-III	Skeleton	60	21	19		
P2b-II	Skeleton	51	28	21		
P2b-I	Skeleton	80	15	5		

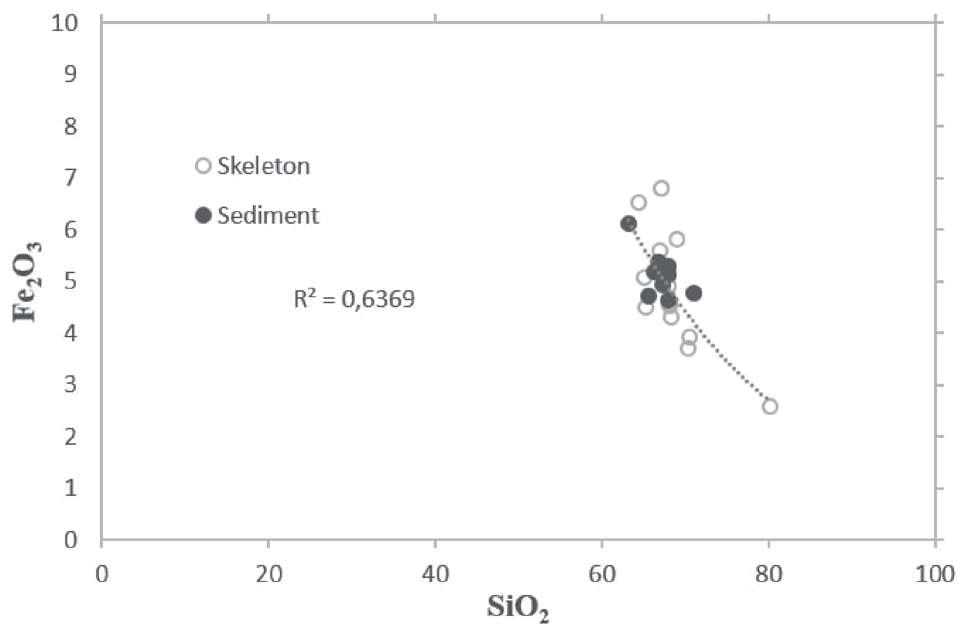

Fig. 9 Statistical relationship between silica and iron in all samples (fine matrix and skeleton). Gradual quartz leaching in conjunction with iron enrichment seems to be an important chemical weathering aspect.

noteworthy, displaying the most weathered rock sample at Blåhø, respectively Rundhø. This indicates more severe exposure to weathering than other horizons. Several authors (e.g. Lautridou and Seppälä 1986; Whalley et al. 2004) have provided information about very low physical weathering intensities under present climate. As such, recent weathering intensity seems to be too weak to produce fines (< 0.063 mm) and too slow to reach the weathering states of our profiles (Whalley et al. 2004). Further, our clay/silt ratios indicate a low chemical weathering (Goodfellow 2012). Accepting the findings of Rea et al. (1996), a post-LGM formation of our profiles with a depth of more than one meter must be questioned. Our grain sizes draw a contrary picture of the expected little soil development in this environment (Darmody and Thorn 1997; Darmody et al. 2000). The relatively high quantity of fine matrix can be explained by sufficient time for production through repeated glacial-interglacial cycles (Goodfellow et al. 2009). The presence of soil horizons, relatively high amount of fine matrix and lichen cover indicate that periglacial surface processes are largely inactive (Goodfellow et al. 2009), especially at P1. It could seem surprising how fine material beneath the blockfield is not largely eroded. A gently dipped autochthonous blockfield protects for the underlying soil matrix and partly hinders erosional processes (Boelhouwers 2004), other authors (see Goodfellow 2007) show that blockfields inherit pre-Holocene material. At road cuts around Rundhø till is visible about three meters below the autochthonous and sorted surface rocks. This shows the past and relict glacial influence. Interpretations of Rundhø pits is far from straightforward as the slope angle leads to disturbance within the soil. The presence of blockstreams indicates at least relict permafrost influence (Goldthwait 1976). This is sustained by Farbrot et al. (2011) who detected seasonal permafrost in a depth down to ~7.5 m and permanent permafrost at least above 1560 m a.s.l. The observed cryogenic influence (cryoturbation soil pocket) at P1-V support the assumption that thermal conditions at the study site allow cryogenic processes to act. These can only act in this way, however, when the area was not ice covered. Based on this consideration our profiles seem to inherit a complex and long history probably extending beyond the Holocene.

5.2 Chronology and considerations about cold-based ice

South-central Norway's landscape history is largely influenced by glacial activity, thick till deposits were detected in and around Gudbrandsdalen (Bergersen and Garnes 1981). During the last major Quaternary glaciation ice flow directions changed, Bergersen and Garnes (1983) postulated four main phases of glaciation. During the initial glaciation phase, Ottadalen and Gudbrandsdalen were influenced by south-westerly ice flow from Jotunheimen which later changed to north-western flow direction during an early phase of the LGM where most till was deposited and a north-eastern flow during the YD. With the ice flow, also the ice divide migrated during the initial phase from north east of the study site, 150 km to the south west, crossing Blåhø, offering the possibility of a thin ice cover. Summits were ice free very early during deglaciation (see Bergersen and Garnes 1983, Figure 34).

The presence of relict landforms in Scandinavia is often explained by the presence of cold-based ice (e.g. Kleman 1994). Sollid and Sørbel (1994) identify former cold-based ice coverage by meltwater channels cutting through blockfields and drumlinoid landforms existing independently to topography indicating a thick ice sheet. Further, Sollid and Sørbel (1994) suggest a warm-based glacier becoming cold-based. This would indicate the incorporation of non-local material transported subglacially. However, we neither detected meltwater channels cutting through blockfields, nor non-local lithology. The consistent lower blockfield boundary in the region is often interpreted as an englacial boundary between cold and warm-based ice but this is unlikely as the thermal boundary should not be parallel to the ice surface (Nesje et al. 1987; Nesje and Dahl 1990).

In contrast to the postulated preservation ability of cold-based ice, it can act as an erosive agent as shown at a thin valley glaciers (Echelmeyer and Zhongxiang 1987; Astakhov et al. 1996). This is supported by Steer et al. (2012), who claim that not only fjords but also high-elevation low-relief surfaces contributed to erosion. Therefore, complete landform preservation without disturbing the surface setting cannot be ensured. Southern Scandinavia was uplifted 1000–1500 m in the Paleogene and 1000 m in the Neogene (Riis 1996). Subsequently, Neogene erosion removed 800–1000 m near the coast. Surface lowering probably more than 100 meters within the Quaternary has to be considered (Steer et al. 2012). The present uplift is estimated 2–3 mm/yr (Fjeldskaar et al. 2000).

The Dye-3 ice core data from Greenland confirm lower annual precipitation during the LGM than during the Holocene for southern Norway (Paterson and Hammer 1987). Almost permanent ice masses in the Norwegian Sea and North Atlantic, moving Atlantic cyclones southward effectively reduced the primary origin of precipitation (Nesje et al. 1988). The little precipitation nowadays is comparable to the precipitation during glacials, supporting the emergence of only thin ice sheets (Dahl et al. 2004). Mangerud (2004) point out that sufficient precipitation is an important factor in the build-up of cold-based ice. We argue that the combination of little precipitation and its key role for cold-based ice build-up, prevented the development of a thick ice sheet in south-central Norway in the Late Weichselian.

Terrestrial cosmogenic nuclide data presented by Goehring et al. (2008) are the main argument for LGM cold-based ice on Blåhø. Their exposure age (25.1 ± 1.8 ^{10}Be ka) from the summit is based on a single erratic and do not take into account erosion or snow shielding, leading to age underestimation (Lal 1991; Gosse and Phillips 2001; Stroeven et al. 2016). As erosion was neglected exposure ages can only yield minimum ages (Dunai 2010). The accuracy of cosmogenic nuclide ages is yet to be improved, the discrepancies in the production of ^{10}Be is around 40% (Gosse and Phillips 2001). In agreement with Ballantyne (1998) we thus state that erratics could have derived from earlier glaciations of unknown age. Moreover, erratic exposure ages are interpreted equivalent to deglaciation (Stroeven et al. 2006), based on the unconfirmed assumption that Blåhø was glaciated. Other expected evidence for cold-based ice refer to the existence of lateral channels, till and scoured bedrock (Sugden and Watts 1977; Dyke 1993). In contrary, all characteristics are absent in the summit area. Bringing together the mentioned findings, in situ cold-based ice formation on Blåhø during the LGM is unlikely. A warm-based ice sheet, instead, which might have frozen to the substratum, becoming cold-based would have demanded the presence of glacially transported material in the profiles which we did not detect. Therefore, precluding cold and warm-based ice, our results cannot exclude the nunatak theory during the LGM, despite the largely accepted cold-based ice theory in Fennoscandia.

5.3 Soil profile chronology

Beside the above mentioned considerations our soil horizons seem to inherit a long and complex history. We applied the growth rate from Matthews (2005), for the mean of the five largest lichens. Ages of 462 yr (P1), respectively 463 yr (P2) are estimated (Table 5). The range of error is complicated to determine as we are applying an existing growth rate with an estimated overall error of 62 ± yr (Matthews 2005), and our measurements bear a 95% confidence interval in years of 462 ± 24.9 yr (P1) and 463 ± 11.6 yr (P2). As local micro-conditions are more important than climate, a slower growth rate (Trenbirth and Matthews 2010) should be considered; in our case due to the low precipitation sums in the study area. It has to be noted that there are many uncertainties involved in lichenometry, e.g. mortality due to snow, the radial growth of lichens, their growth behavior in general, and the influence of competition (e.g. Osborn et al. 2015; Armstrong 2016). We used the successful applied growth rate and the assumptions made by Matthews (2005), being aware that other studies use different assumptions (see Osborn et al. 2015).

Tab. 5 Lichenometric dating, ages calculated with growth rate of 0.45 mm/yr (Matthews 2005)

Five largest lichens	P1	P2
Mean (mm)	208.0	208.2
Median (mm)	233	210
Standard deviation	44.5	20.86
Standard error of the mean	19.9	9.32
Confidence interval of the mean (95%)	55.3	25.9
Estimated age (yr)	462.0	463.0

Our histograms indicate a complex colonization history, and the high number of small lichens is noteworthy. The skewed nature of the lichen distribution could reflect delayed or different phases of colonization (Roberts et al. 2010), stressing the longevity of the population. The measured diameters larger than 140 mm indicate to predate the Little Ice Age (LIA) (Matthews and Shakesby 1984). As our largest individuals are supposed to be relatively old, the amount of smaller specimen show that the lichen community is dynamic, reproducing and that our estimated ages are not unrealistic. Ages of P1 are considered to be more reliable due to flat topography and surface arrangement. Lichens at northern exposure from P1 might be older than from P2, experiencing longer lying snow and less insolation, lichens at P1 need more time to reach the same thalli diameter (Griffey 1977). The range lichenometric dating is sufficient for our study to determine, if the surface was disturbed by the LIA. Due to Osborn et al. (2015), this is possible by using large Rhizocarpon thalli. The Neoglacial peak during the LIA which was observed at many Norwegian glaciers (Nesje 2009) did not glacially influence our study site. There is no indication that the blockfield influenced by glacial activity post-dating the rock shattering. The surface is dominated by angular rocks without structural orientation from glacial influence. Cook-Talbot (1991) shows that surface clasts surviving the LIA are stable for several hundred years. The most severe climate detoriation predating the LIA is the Younger Dryas (YD) which might have altered the landscape. Follestad (2007) mapped YD moraines up to 1400–1500 m a.s.l. approximately 50 km north of our study site, which can be interpreted as the YD ice surface. This observation and including the lack of glacial erosion, we assume that Blåhø was not affected by the YD. Goehring et al. (2008) investigated erratic boulders on Blåhø from 1086 and 1182 m a.s.l. representing quick ice sheet lowering from 15.0 to 11.7 ka., supporting no ice cover at the summit during YD. Hence, we consider minimum blockfield surface stability since at least 12.5 kyr.

Consequently, P1-VI is exposed to the surface since at least 12.5 kyr, this is supported by the high proportion of sand inducing continued aeolian processes removing smaller fractions and high LOI content which incorporates organic content from the climate amelioration ~7.5 to 6.4–6.1 kyr (Paus et al. 2011). The properties of P1-V concerning the weathering indices, the leaching of trace elements, the high silt volumes, and its dark upper part appear to reflect the Eemian interstadial (MIS 5e, 130–115 kyr). MIS 5e is the only eligible period in terms of temperature and duration which might have caused the profile characteristics. The periglacial involution reflected in the upper part of P1-V might have taken place during the climatic cooling (French 2007) after the Eemian towards MIS 2 (LGM). We thus argue that the lower part of P1-V marks the transition between MIS 6 to MIS 5 with slowly increasing temperatures indicated by higher organic content in the profile. Probably P1-IV represents the periods from MIS 9 to MIS 6 (337–130 kyr) with continuously cold temperatures and only minor periods of climatic amelioration. This assumption is sustained by lighter color, lower organic content and lower abundance of sand. The low amount of sand might evolve from slow chemical weathering during long-term cold conditions causing relatively fresh CIA and WIP values. The dark layer of the upper part of P1-III and P1-II must have developed in earlier interglacials. Further exploration of the age of the blockfield by cosmogenic nuclides exposure age dating is in progress.

Concluding, all our site related information point to the fact that blockfields in south-central Norway were not generally covered by cold-based ice during recent glaciations. We argue that the prerequisites for build-up a cold-based ice cap were not given in the area during recent glaciations. Furthermore, the profile properties indicate a long chemical weathering history under changing environmental conditions. Therefore, cold-based ice coverage cannot conclusively be excluded, but appears to be unlikely.

Acknowledgements

We are thankful to Simone Ackermann who provided expertise in field and lab. Furthermore, we thank the Svare family for support. We are also grateful to the Steinmann-Institute, University of Bonn for the support in the laboratory, special thanks to Dr. Sven-Oliver Franz. Thanks to Camilla Kurth for assistance and advices in our laboratory. We thank the Friedrich-Ebert-Stiftung for their financial support. We also thank two reviewers for improving the paper significantly.

REFERENCES

ALLEN, C. E., DARMODY, R. G., THORN, C. E., DIXON, J. C., SCHLYTER, P. (2001): Clay mineralogy, chemical weathering and landscape evolution in Arctic-Alpine Sweden. Geoderma 99, 277–294. https://doi.org/10.1016/S0016-7061(00)00075-6

ARMSTRONG, R. A. (2011): The biology of the crustose lichen *Rhizocarpon geographicum*. Symbiosis 55(2), 53–68. https://doi.org/10.1007/s13199-011-0147-x

ARMSTRONG, R. A. (2016): Invited review: Lichenometric dating (lichenometry) and the biology of the lichen genus Rhizocarpon: challenges and future directions. Geografiska Annaler A Physical Geography 98(3), 183–206. https://doi.org/10.1111/geoa.12130

ASTAKHOV, V. I., KAPLYANSKAYA, F. A., TARNOGRADSKY, V. D. (1996): Pleistocene permafrost of West Siberia as a deformable glacier bed. Permafrost and Periglacial Processes 7(2), 165–191. https://doi.org/10.1002/(SICI)1099-1530(199604)7:2<165::AID-PPP218>3.0.CO;2-S

BALLANTYNE, C. K., MCCARROLL, D., NESJE, A., DAHL, S. O. (1997): Periglacial trimlines, former nunataks and the altitude of the last ice sheet in Wester Ross, northwest Scotland. Journal of Quaternary Science 12(3), 225–238. https://doi.org/10.1002/(SICI)1099-1417(199705/06)12:3<225::AID-JQS302>3.0.CO;2-A

BALLANTYNE, C. K. (1998): Age and Significance of Mountain-Top Detritus. Permafrost and Periglacial Processes 9(4), 327–345. https://doi.org/10.1002/(SICI)1099-1530(199810/12)9:4<327::AID-PPP298>3.0.CO;2-9

BALLANTYNE, C. K. (2010): A general model of autochthonous blockfield evolution. Permafrost and Periglacial Processes 21(4), 289–300. https://doi.org/10.1002/ppp.700

BENEDICT, J. B. (1967): Recent glacial history of an alpine area Colorado Front Range, U.S.A. I. Establishing lichen-growth curve. Journal of Glaciology 6(48), 817–832. https://doi.org/10.3189/S0022143000020128

BERGERSEN, O. F., GARNES, K. (1981): Weichselian in central South Norway: the Gudbrandsdal Interstadial and the following glaciation. Boreas, pp. 315–322. https://doi.org/10.1111/j.1502-3885.1981.tb00493.x

BERGERSEN, O. F., GARNES, K. (1983): Glacial deposits in the culmination zone of the Scandinavian ice sheet. In EHLERS, J. (ed.): Glacial deposits in north-west Europe, pp. 23–40. Balkema, Rotterdam, Holland.

BESCHEL, R. E. (1961): Dating Rock Surfaces by Lichen Growth and its Application to Glaciology and Physiography (Lichenometry). Geology of the Arctic, pp. 1044–1062.

BIRKELAND, P. W. (1999): Soil and Geomorphology. Oxford University Press, New York.

BLYTT, A. (1876): Immigration of the Norwegian Flora. Alb. Cammermeyer, Christiania.

BOELHOUWERS, J. (2004): New perspective on autochthonous blockfield development. Polar Geography 28(2), 133–146. https://doi.org/10.1080/789610122

BRADWELL, T. (2009): Lichenometric dating: A commentary, in the light of some recent statistical studies. Geografiska Annaler A Physical Geography 91(2), 61–69. https://doi.org/10.1111/j.1468-0459.2009.00354.x

BROOK, E. J., NESJE, A., LEHMAN, S. J., RAISBECK, G. M., YIOU, F. (1996): Cosmogenic nuclide exposure ages along a vertical transect in western Norway: Implications for the height of the Fennoscandian ice sheet. Geology 24(3), 207–210. https://doi.org/10.1130/0091-7613(1996)024<0207:CNEAAA>2.3.CO;2

COOK-TALBOT, J. D. (1991): Sorted circles, relative-age dating and palaeoenvironmental reconstruction in an alpine periglacial environment, eastern Jotunheimen, Norway: lichenometric and weathering-based approaches. The Holocene 1(2), 128–141. https://doi.org/10.1177/095968369100100205

DAHL, R. (1966): Block Fields, Weathering Pits and Tor-like Forms in the Narvik Moun-tains, Nordland, Norway. Geografiska Annaler. Series A, Physical Geography 48(2), 55–85. https://doi.org/10.2307/520419

DAHL, S. O., NESJE, A., ØVESTDAL, J. (1997): Cirque glaciers as morphological evidence for a thin Younger Dryas ice sheet in east-central southern Norway. Boreas 26(3), 161–180. https://doi.org/10.1111/j.1502-3885.1997.tb00850.x

DAHL, S. O., LIE, Ø., PYTTE, A.-G. B., MURRAY, A., TVERANGER, J., HÅVIK, O., KVISVIK, B. C., NESJE, A. (2004): Weichselian glaciation history in east-central southern Norway. Geografiske Föreningnes Förhandlingar 126, 118–119.

DARMODY, R. G., THORN, C. E. (1997): Elevation, age, soil development, and chemical weathering at Storbreen, Jotunheimen, Norway. Geografiska Annaler. Series A, Physical Ge-ography 79A, 15–222. https://doi.org/10.1111/1468-0459.00018

DARMODY, R. G., THORN, C. E., DIXON, J. C., SCHLYTER, P. (2000): Soils and land-scapes of Kärvagge, Swedish Lapland. Soil Science Society of America 64(4), 1455–1466. https://doi.org/10.2136/sssaj2000.6441455x

DARMODY, R. G., THORN, C. E., ALLEN, C. E. (2005): Chemical weathering and boulder mantles, Kärkevagge, Swedish Lapland. Geomorphology 67, 159–170. https://doi.org/10.1016/j.geomorph.2004.07.011

DENTON, G. H., HUGHES, I. J. (1981): The Last Great Ice Sheets. John Wiley, New York.

DREDGE, L. (1992): Breakup of limestone bedrock by frost shattering and chemical weather-ing. Eastern Canadian Arctic. Arctic Alpine Research 24(4), 314–323. https://doi.org/10.2307/1551286

DUNAI, T. J. (2010): Cosmogenic Nuclides: Principles, Concepts and Applications in the Earth Surface Sciences. Cambridge University Press, Cambridge.

DYKE, A. S. (1993): Landscapes of cold-centred Late Wisconsinan ice caps, Arctic Canada. Progress in Physical Geography 17(2), 223–247. https://doi.org/10.1177/030913339301700208

ECHELMEYER, K., ZHONGXIANG, W. (1987): Direct observation of basal sliding and deformation of basal drift at sub-freezing temperatures. Journal of Glaciology 33(113), 83–98. https://doi.org/10.3189/S0022143000005396

FARBROT, H., HIPP, T. F., ETZELMÜLLER, B., ISAKSEN, K., ØDEGÅRD, R. S., SCHULER, T. V., HUMLUM, O. (2011): Air and Ground Temperature Variations Observed along Elevation and Continentality Gradients in Southern Norway. Permafrost and Periglacial Processes 22(4), 343–360. https://doi.org/10.1002/ppp.733

FJELLANGER, J., SØRBEL, L., LINGE, H., BROOK, E. J., RAISBECK, G. M., YIOU, F. (2006): Glacial survival of blockfields on the Varanger Peninsula, northern Norway. Geomorphology 82, 255–272. https://doi.org/10.1016/j.geomorph.2006.05.007

FJELDSKAAR, W., LINDHOLM, C. DEHLS, J. F., FJELDSKAAR, I. (2000): Postglacial uplift, neotectonics and seismicity in Fennoscandia. Quaternary Science Reviews 19, 1413–1422. https://doi.org/10.1016/S0277-3791(00)00070-6

FRENCH, H. M. (2007): The Periglacial Environment. 3rd ed. Wiley, Chichester. https://doi.org/10.1002/9781118684931

FOLLESTAD, B. (1990): Block fields, ice-flow directions and the Pleistocene ice sheet in Nordmøre and Romsdal, West Norway. Norsk Geografisk Tidsskrift – Norwegian Journal of Geography 70, 27–33.

FOLLESTAD, B. (2003): Development of minor late-glacial ice domes east of Oppdal, Central Norway. Norges geologiske undersøkelse Bulletin 441, 39–49.

FOLLESTAD, B. (2007): Lesjakog 1419 III. Preliminært kvartærgeologisk kart I M 1:50.000. Norges geologiske undersøkelse.

GRIFFEY, N. J. (1977): A lichenometric study of the Neoglacial end moraines of the Okstindan Glaciers, North Norway, and comparisons with similar recent Scandinavian studies. Norsk geografisk Tidsskrift – Norwegian Journal of Geography 31(4), 163–172. https://doi.org/10.1080/00291957708552019

GOEHRING, B. M., BROOK, E. J., LINGE, H., RAISBECK, G. M., YIOU, F. (2008): Beryllium-10 exposure ages of erratic boulders in southern Norway and implications for the history of the Fennoscandian Ice Sheet. Quaternary Science Reviews 27, 320–336. https://doi.org/10.1016/j.quascirev.2007.11.004

GOLDWHAYT, R. P. (1976): Frost-sorted patterned ground: a review. Quaternary Research 6(1), 27–35. https://doi.org/10.1016/0033-5894(76)90038-7

GOODFELLOW, B. W. (2007): Relict non-glacial surfaces in formerly glaciated landscapes. Earth-Science Reviews 80, 47–73. https://doi.org/10.1016/j.earscirev.2006.08.002

GOODFELLOW, B. W. (2012): A granulometry and secondary mineral fingerprint of chemical weathering in periglacial landscapes and its application to blockfield origins. Quaternary Science Reviews 57, 121–135. https://doi.org/10.1016/j.quascirev.2012.09.023

GOODFELLOW, B. W., FREDIN, O., DERRON, M.-H., STROEVEN, A. P. (2009): Weathering processes and Quaternary origin of an alpine blockfield in Arctic Sweden. Boreas 38, 379–398. https://doi.org/10.1111/j.1502-3885.2008.00061.x

GOSSE, J. C., PHILLIPS, F. M. (2001): Terrestrial in situ cosmogenic nuclides: theory and application. Quaternary Science Reviews 20, 1475–1560. https://doi.org/10.1016/S0277-3791(00)00171-2

GOUVEIA, M. A., PRUDÊNCIO, M. I., FIGUEIREDO, M. O., PEREIRA, L., WAERENBORGH, J. C., MORGADO, I., PENA, T., LOPES, A. (1993): Behavior of REE and other trace and major elements during weathering of granitic rocks, Évora, Portugal. Chemical Geology 107, 293–296. https://doi.org/10.1016/0009-2541(93)90194-N

GRANT, J. A. (2005): Isocon analysis: A brief review of the method and application. Physics and Chemistry of the Earth 30, 997–1004. https://doi.org/10.1016/j.pce.2004.11.003

HALL, K., THORN, C. E., MATSUOKA, N., PRICK, A. (2002): Weathering in cold regions: some thoughts and perspectives. Progress in Physical Geography 26(4), 577–603. https://doi.org/10.1191/0309133302pp353ra

HARRIS, C., CASELDINE, C. J., CHAMBERS, W. J. (1987): Radiocarbon dating of a palaeosol buried by sediments of a former ice-dammed lake. Leirbreen, southern Norway. Norsk Geografisk Tidsskrift – Norwegian Journal of Geography 41(2), 81–90. https://doi.org/10.1080/00291958708621982

HEIRI, O., LOTTER, A. F., LEMCKE, G. (2001): Loss on ignition as a method for estimating organic and carbonate content in sediments: reproducibility and comparability of results. Journal of Paleolimnology 25(1), 101–110. https://doi.org/10.1023/A:1008119611481

JOCHIMSEN, M. (1973): Does the size of lichen thalli really constitute a valid measure for da-ting glacial deposits? Arctic and Alpine Research 5(4), 417–424. https://doi.org/10.2307/1550132

KLEMAN, J. (1994): Preservation of landforms under ice sheets and ice caps. Geomorphology 9, 19–32. https://doi.org/10.1016/0169-555X(94)90028-0

KLEMAN, J., BORGSTROM, I. (1990): The Boulder Fields of Mt. Fulufjallet, West-Central Sweden – Late Weichselian Boulder Blankets and Interstadial Periglacial Phenomena. Geografiska Annaler. Series A, Physical Geography 72(1), 63–78. https://doi.org/10.2307/521238

KLEMAN, J., STROEVEN, A. P. (1997): Preglacial surface remnants and Quaternary glacial regimes in northwestern Sweden. Geomorphology 19, 35–54. https://doi.org/10.1016/S0169-555X(96)00046-3

KLEMAN, J., HATTESTRAND, C., BORGSTROM, I., STROEVEN, A. (1997): Fennoscandian palaeoglaciology reconstructed using a glacial geological inversion model. Journal of Glaciology 43(144), 283–299. https://doi.org/10.3189/S0022143000003233

LAGERBÄCK, R. (1988): Periglacial phenomena in the wooded areas of Northern Sweden – relicts from the Tärendö Interstadial. Boreas 17(4), 487–499. https://doi.org/10.1111/j.1502-3885.1988.tb00563.x

LAL, D. (1991): Cosmic ray labeling of erosion surfaces: in situ nuclide production rates and erosion rates. Earth and Planetary Science Letters 104, 424–439. https://doi.org/10.1016/0012-821X(91)90220-C

LANDVIK, J. Y., BROOK, E. J., GUALTIERI, L., RAISBECK, G. M., SALVIGSEN, O., YIOU, F. (2003): Northwest Svalbard during the last glaciation: Ice-free areas existed. Geology 31(10), 905–908. https://doi.org/10.1130/G19703.1

LAUTRIDOU, J. P., SEPPÄLÄ, M. (1986): Experimental Frost Shattering of Some Precambrian Rocks, Finland. Geografiska Annaler A Physical Geography 68(1/2), 89–100. https://doi.org/10.2307/521179

LINGE, H., BROOK, E. J., NESJE, A., RAISBECK, G. M., YIOU, F., CLARK, H. (2006): In situ ^{10}Be exposure ages from southeastern Norway: implications for the geometry of the Weichselian Scandinavian ice sheet. Quaternary Science Reviews 25, 1097–1109. https://doi.org/10.1016/j.quascirev.2005.10.007

MANGERUD, J. (1991): The Last Ice Age in Scandinavia. In: ANDERSEN, B. G., KÖNIGSSON, L. K. (eds.): Late Quaternary Stratigraphy in the Nordic Countries 150,000–15,000 B.P. (15–30). Uppsala.

MANGERUD, J. (2004): Ice sheet limits in Norway and on the Norwegian continental shelf. In: EHLERS, J., GIBBARD, P. L. (eds.): Quaternary Glaciations – Extent and Chronology. Part I: Europe (271–294). Amsterdam, Elsevier. https://doi.org/10.1016/S1571-0866(04)80078-2

MARKL, G., MARKS, M. (2008): Minerale und Gesteine. Mineralogie – Petrographie – Geochemie. Heidelberg, Neckar, Spektrum Akademischer Verlag.

MARQUETTE, G. C., GRAY, J. T., GOSSE, J. C., COURCHESNE, F., STOCKLI, L., MACPHERSON, G., FINKEL, R. (2004): Felsenmeer persistence under non-erosive ice in the Torngat and Kaumajet mountains, Quebec and Labrador, as determined by soil weathering and cosmogenic nuclide exposure dating. Canadian Journal of Earth Sciences 41(1), 19–38. https://doi.org/10.1139/e03-072

MATTHEWS, J. A., SHAKESBY, R. A. (1984): The status of the 'Little Ice Age' in southern Norway: relative-age dating of Neoglacial moraines with Schmidt hammer and lichenometry. Boreas 13(3), 333–346. https://doi.org/10.1111/j.1502-3885.1984.tb01128.x

MATTHEWS, J. A. (1994): Lichenometric Dating: A review with particular reference to 'Little Ice Age' moraines in southern Norway. In: BECK, C. (eds.): Dating in exposed and surface con-texts (185–212). Albuquerque, University of New Mexico Press.

MATTHEWS, J. A. (2005): 'Little Ice Age' glacier variations in Jotunheimen, southern Norway: a study in regionally controlled lichenometric dating of recessional moraines with implications for climate and lichen growth rates. The Holocene 15(1), 1–19. https://doi.org/10.1191/0959683605hl779rp

MAYNARD, J. B. (1992): Chemistry of modern soils as a guide to interpreting Precambrian paleosols. The Journal of Geology 100(3), 279–289. https://doi.org/10.1086/629632

MOEN, A. (1998): Nasjonalatlas for Norge: vegetasjon (National atlas of Norway: vegetation). Norwegian Mapping Authority. Hønefoss, Norway.

MUNSELL, C. (1994): Munsell soil color charts. Macbeth Division of Kollmorgen Instruments Corporation, New Windsor.

NESBITT, H. W., YOUNG, G. M. (1982): Early Proterozoic climates and plate motions inferred from major element chemistry of lutites. Nature 299, 715–717. https://doi.org/10.1038/299715a0

NESJE, A., ANDA, E., RYE, N., LIEN, R., HOLE, P. A., BLIKRA, L. H. (1987): The vertical extent of the Late Weichselian ice sheet in the Nordfjord–Møre area, western Norway. Norsk Geografisk Tidsskrift – Norwegian Journal of Geography 67, 125–141.

NESJE, A., DAHL, S. O., RYE, E. A., RYE, N. (1988): Block fields in southern Norway: Significance for the late Weichselian ice sheet. Norsk Geografisk Tidsskrift – Norwegian Journal of Geography 68, 149–169.

NESJE, A., DAHL, S. O. (1990): Autochthonous block fields in southern Norway: Implications for the geometry, thickness, and isostatic loading of the Late Weichselian Scandinavian ice sheet. Journal of Quaternary Science 5(3), 225–234. https://doi.org/10.1002/jqs.3390050305

NESJE, A., MCCARROLL, D., DAHL, S. O. (1994): Degree of rock surface weathering as an indicator of ice-sheet thickness along an east-west transect across southern Norway. Journal of Quaternary Science 9(4), 337–347. https://doi.org/10.1002/jqs.3390090404

NESJE, A., DAHL, S. O., LINGE, H., BALLANTYNE, C. K., MCCARROLL, D., BROOK, E. J., RAISBECK, G. M., YIOU, F. (2007): The surface geometry of the Last Glacial Maximum ice sheet in the Andøya-Skånland region, northern Norway, constrained by surface exposure dating and clay mineralogy. Boreas 36(3), 227–239. https://doi.org/10.1111/j.1502-3885.2007.tb01247.x

NESJE, A. (2009): Latest Pleistocene and Holocene alpine glacier fluctuations in Scandinavia. Quaternary Science Reviews 28, 2119–2136. https://doi.org/10.1016/j.quascirev.2008.12.016

OSBORN, G., MCCARTHY, D., LABRIE, A., BURKE, R. (2015): Lichenometric dating: Science or pseudo-science? Quaternary Research 83(1), 1–12. https://doi.org/10.1016/j.yqres.2014.09.006

PAPE, R., LÖFFLER, J. (2017): Determinants of arctic-alpine pasture resources: the need for a spatially and functionally fine-scaled perspective. Geografiska Annaler: Series A, Physical Geography. https://doi.org/10.1080/04353676.2017.1368833

PARKER, A. (1970): An index of weathering for silicate rocks. Geological Magazine 107(6), 501–504. https://doi.org/10.1017/S0016756800058581

PATERSON, W. S. B., HAMMER, C. U. (1987): Ice core and other glaciological data. In: RUDDIMAN, W. F., WRIGHT JR., H. E. (eds.): North America and Adjacent Oceans During the last Deglaciation (91–109). Boulder, CO., Geological Society of America. https://doi.org/10.1130/DNAG-GNA-K3.91

PAUS, A., VELLE, G., BERGE, J. (2011): The Lateglacial and early Holocene vegetation and environment in the Dovre mountains, central Norway, as signalled in two Lateglacial nunatak lakes. Quaternary Science Reviews 30, 1780–1796. https://doi.org/10.1016/j.quascirev.2011.04.010

PRICE, J. R., VELBEL, M. A. (2003): Chemical weathering indices applied to weathering profiles developed on heterogeneous felsic metamorphic parent rocks. Chemical Geology 202, 397–416. https://doi.org/10.1016/j.chemgeo.2002.11.001.

RAPP, A. (1960): Recent development of mountain slopes on Kärkevagge and surroundings, northern Scandinavia. Geografiska Annaler A Physical Geography 42(2/3), 65–200. https://doi.org/10.2307/520126

REA, B. R., WHALLEY, W., RAINEY, M. M., GORDON, J. E. (1996): Blockfields, old or new? Evidence and implications from some plateaus in northern Norway. Geomorphology 15, 109–121. https://doi.org/10.1016/0169-555X(95)00118-O

ROBERTS, S. J., HODGSON, D. A., SHELLEY, S., ROYLES, J., GRIFFITHS, H. J., DEEN, T. J., THORNE, M. A. S. (2010): Establishing lichenometric ages for nineteenth- and twentieth-century glacier fluctuations on South Georgia (South

Atlantic). Geografiska Annaler A Physical Geography 92(1), 125–139. https://doi.org/10.1111/j.1468-0459.2010.00382.x

RIIS, F. (1996): Quantification of Cenozoic vertical movements of Scandinavia by correlation of morphological surfaces with offshore data. Global and Planetary Change 12, 331–357. https://doi.org/10.1016/0921-8181(95)00027-5

SCHAEFER M. J., FINKEL, R. C., BALCO, G., ALLEY, R. B., CAFFEE, M. W., BRINER, J. P., YOUNG, N. E., GOW, A. J., SCHWARTZ, R. (2016): Greenland was nearly ice-free for extended periods during the Pleistocene. Nature 540, 252–255. https://doi.org/10.1038/nature20146

SEJRUP, H.P., NYGÅRD, A., HALL, A. M., HAFLIDASON, H. (2009): Middle and Late Weichselian (Devensian) glaciation history of south-western Norway, North Sea and eastern UK. Quaternary Science Reviews 28, 370–380. https://doi.org/10.1016/j.quascirev.2008.10.019

SHAKESBY, R. A., MATTHEWS, J. A., WINKLER, S. (2004): Glacier variations in Breheimen, southern Norway: relative-age dating of Holocene moraine complexes at six high-altitude glaciers. The Holocene 14(6), 899–910. https://doi.org/10.1191/0959683603hl766rp

SHELDON, N. D., TABOR, N. J. (2009): Quantitative paleoenvironmental and paleoclimatic reconstruction using paleosols. Earth-Science Reviews 95, 1–52. https://doi.org/10.1016/j.earscirev.2009.03.004

SIGMOND, E. M. O., GUSTAVSON, M., ROBERTS, D. (1984): Bergrunnskart over Norge. Scale 1:1 million. Norges Geologiske Undersøkelse.

SOLLID, J. L., SØRBEL, L. (1994): Distribution of Glacial Landforms in Southern Norway in Relation to the Thermal Regime of the Last Continental Ice Sheet. Geografiska Annaler A Physical Geography 76(1/2), 25–35. https://doi.org/10.2307/521317

STEER, P., HUISMANS, R.S., VALLA, P.G., GAC, S., HERMAN, F. (2012): Bimodal Plio-Quaternary glacial erosion of fjords and low-relief surfaces in Scandinavia. Nature Geoscience 5, 635–639. https://doi.org/10.1038/ngeo1549

STROEVEN, A. P., HARBOR, J., FABEL, D., KLEMAN, J., HÄTTESTRAND, C., ELMORE, D., FINK, D., FREDIN, O. (2006): Slow, patchy landscape evolution in northern Sweden despite repeated ice-sheet glaciation. In: WILLETT, S. D., HOVIUS, N., BRANDON, M. T., FISHER, D. M. (eds.): Tectonics, Climate, and Landscape Evolution: Geological Society of America Special Paper 398, Penrose Conference Series, pp. 387–396. https://doi.org/10.1130/2006.2398(24)

STROEVEN, A. P., HÄTTESTRAND, C., KLEMAN, J., HEYMAN, J., FABEL, D., FREDIN, O., GOODFELLOW, B. W., HARBOR, J. M., JANSEN, J. D., OLSEN, L., CAFFEE, M. W., FINK, D., LUNDQVIST, J., ROSQVIST, G. C., STRÖMBERG, B., JANSSON, K. N. (2016): Deglaciation of Fennoscandia. Quaternary Science Reviews 147, 91–121. https://doi.org/10.1016/j.quascirev.2015.09.016

STRØMSØE, J. R., PAASCHE, Ø. (2011): Weathering patterns in high-latitude regolith. Journal of Geophysical Research 116(F3), 1–17. https://doi.org/10.1029/2010JF001954.

SUGDEN, D. E., WATTS, S. H. (1977): Tors, felsenmeer, and glaciation in northern Cumberland Peninsula, Baffin Island. Canadian Journal of Earth Sciences 14(12), 2817–2823. https://doi.org/10.1139/e77-248

SUGDEN, D. E., WATTS S. H. (1978): Glacial erosion by the Laurentide ice sheet. Journal of Glaciology 20(83), 367–391. https://doi.org/10.3189/S0022143000013915

TRENBIRTH, H. E. (2010): Lichenometry. In: CLARKE, L. E., NIELD, J. M. (eds.): Geomorphological Techniques (Online Edition) (1–12). London, British Society for Geomorphology.

TRENBIRTH, H. E., MATTHEWS, J. A. (2010): Lichen growth rates on glacier forelands in southern Norway: Preliminary results from a 25-year monitoring programme. Geografiska Annaler A Physical Geography 92(1), 19–39. https://doi.org/10.1111/j.1468-0459.2010.00375.x

TUCKER, M. E. (1996): Methoden der Sedimentologie. 38 Tabellen. Stuttgart, Enke.

WEBBER, P. J., ANDREWS, J. T. (1973): Lichenometry: A comment. Arctic and Alpine Research 5(4), 295–302. https://doi.org/10.2307/1550121

WHALLEY, W. B., REA, B. R., RAINEY, M. M. (2004): Weathering, Blockfields, and Fracture Systems and the Implications for Long–Term Landscape Formation: Some Evidence from Lyngen and Øksfordjøkelen Areas in North Norway. Polar Geography 28(2), 93–119. https://doi.org/10.1080/789610120

WINGUTH, C., MICKELSON, D., LARSEN, E., DARTER, J., MOELLER, C., STALSBERG, K. (2005): Thickness evolution of the Scandinavian Ice Sheet during the Late Weichselian in Nordfjord, western Norway: evidence from ice-flow modeling. Boreas 34, 176–185. https://doi.org/10.1080/03009480510012953

WINKLER, S., MATTHEWS, J. A., SHAKESBY, R. A., DRESSER, P. Q. (2003): Glacier variations in Breheimen, southern Norway: dating Little Ice Age moraine sequences at seven low-altitude glaciers. Journal of Quaternary Science 18(5), 395–413. https://doi.org/10.1002/jqs.756